Table 1 Integration constants V_{fc} corresponding to different insulation thicknesses

V_{fc} ($\times 10^{-2}$)	h ($\times 10^{-2}$ m)
−3.5	3.79
−3.25	3.82
−3.0	3.85
−2.75	3.89
−2.5	3.93
−2.25	3.99
−2.0	4.05
−1.75	4.13
−1.50	4.23
−1.25	4.36
−1.00	4.54

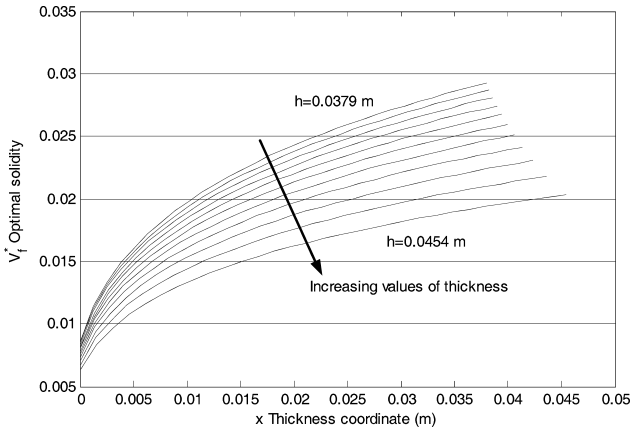

Fig. 3 Optimum solidity profiles for various thickness of insulation.

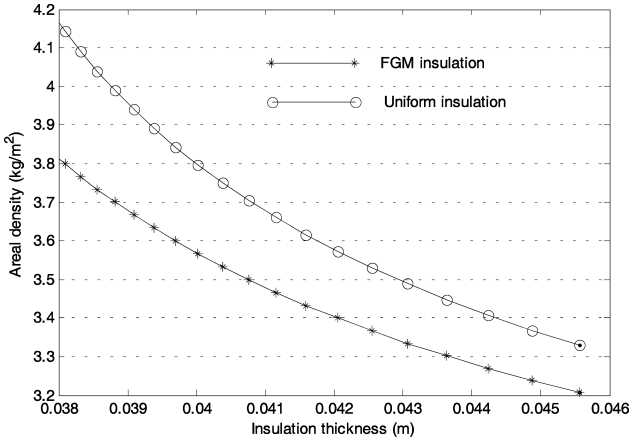

Fig. 4 Comparison of mass per unit area for functionally graded and uniform solidity insulations.

savings are higher for thin insulation with about 8.6% less mass for 3.79 cm and only about 3.6% savings for 4.54 cm.

V. Summary

We studied the problem of one-dimensional steady-state heat conduction in metallic foams used as thermal protection systems with varying density in the thickness direction. The thermal conductivity of the foam is a function of temperature as well as the density, and it has a minimum value in the range of densities of our interest. An optimality criterion in the form of a differential equation was derived in order to minimize the total mass of the insulation for a given heat input. The heat-conduction equation and the optimality equation were solved numerically to obtain optimum density profiles for various values of thickness of the insulation. It is shown that for a given thickness using functionally graded foams can reduce the mass of the insulation panel.

Acknowledgments

This work was funded by the Metals and Thermal Structures Branch at NASA Langley Research Center through Grant NAG-1-01046. Support from NASA URETI Grant NCC3-994 managed by Glenn Research Center is also acknowledged.

References

[1]Ashby, M. F., Evans, A. G., Fleck, N. A., Gibson, L. J., Hutchinson, J. W., and Wadley, H. N. G., *Metal Foams—A Design Guide*, Butterworth–Heinemann, Boston, 2000, pp. 181–188.

[2]Blosser, M. L., "Advanced Metallic Thermal Protection Systems for Reusable Launch Vehicles," Ph.D. Dissertation, Dept. of Mechanical and Aerospace Engineering, Univ. of Virginia, Charlottesville, VA, May 2000.

[3]Bhattacharya, A., Calmidi, V. V., and Mahajan, L. R., "Thermophysical Properties of High Porosity Metal Foams," *International Journal of Heat and Mass Transfer*, Vol. 45, No. 5, 2002, pp. 1017–1031.

[4]Boomsma, K., and Poulikakos, D., "On the Effective Thermal Conductivity of a Three-Dimensional Structured Fluid-Saturated Metal Foam," *International Journal of Heat and Mass Transfer*, Vol. 44, No. 4, 2001, pp. 827–836.

[5]Glicksman, L. R., "Heat Transfer in Foams," *Low Density Cellular Plastics: Physical Basis of Behavior*, edited by N. C. Hilyard and A. Cunningham, Chapman and Hall, London, 1994, pp. 104–139.

[6]Venkataraman, S., Zhu, H., Sankar, B. V., Haftka, R. T., and Blosser, M., "Optimum Design of a Functionally Graded Metallic Foam Thermal Insulation," *Proceedings of the American Society for Composites—16th Annual Technical Conference*, edited by M. W. Hyer, Dept. of Engineering Science and Mechanics, Virginia Polytechnic Inst. and State Univ., Blacksburg, VA, 2001, Paper 127.

W. Williamson
Associate Editor

Multiblock Compressible Navier–Stokes Flow Solver Applied to Complex Launch Vehicles

Abdollah Arabshahi* and J. Mark Janus†
Mississippi State University,
Mississippi State, Mississippi 39762

Introduction

THE development of computational-fluid-dynamics procedures has progressed rapidly during the past two decades. Simultaneously, the rapid development in computer hardware has not only matched the explosive algorithm development but has indeed provided, and continues to provide, its impetus. Together, the computational resources are now available for the numerical simulation of the flow about many complex three-dimensional aerospace configurations. An efficient and accurate flow solver is the key to developing a useful engineering tool for the analysis of complex three-dimensional flow phenomena about complex configurations. Consequently, there is an avid interest in finding solution methodologies that will produce results in less time and cost, compared

Presented as Paper 99-3378 at the 14th Computational Fluid Dynamics Conference, Norfolk, VA, 28 June–1 July 1999; received 15 August 2003; revision received 23 December 2003; accepted for publication 9 January 2004. Copyright © 2004 by the American Institute of Aeronautics and Astronautics, Inc. All rights reserved. Copies of this paper may be made for personal or internal use, on condition that the copier pay the $10.00 per-copy fee to the Copyright Clearance Center, Inc., 222 Rosewood Drive, Danvers, MA 01923; include the code 0022-4650/04 $10.00 in correspondence with the CCC.

*Research Engineer, Computational Simulation and Design Center; currently Associate Research Professor, Graduate School of Computational Engineering, University of Tennessee SimCenter at Chattanooga, 701 East M.L. King Boulevard, Chattanooga, TN 37403. Member AIAA.

†Associate Professor, Department of Aerospace Engineering, Computational Simulation and Design Center, P. O. Drawer A. Senior Member AIAA.

to wind-tunnel tests. A flow solver, UBIFLOW (unsteady blocked implicit FLOW solver), that has been evolving for many years now, was developed for just this purpose. Complex launch-vehicle flow solutions are presented in this work to evaluate the performance of UBIFLOW and to begin establishing its credibility for that type of configuration.

Mathematical and Numerical Formulation

Domain Decomposition Strategy

UBIFLOW uses a structured-grid, blocked domain decomposition allowing nearly unrestricted arrangement of variably sized blocks.[1] In this approach the computational region is decomposed into distinct subregions, each of which is gridded independently. The grid topology for each subregion is locally consistent with each component of the geometry. The code requires C^0 grid line continuity across block boundaries. As a consequence of this requirement, noninterpolated block-block interfaces are a key feature of UBIFLOW. In addition, to accommodate truly generalized time-dependent curvilinear coordinate systems where grid cell deformation is likely, UBIFLOW satisfies the geometric (or space) conservation law.[2]

Governing Equations

For high-Reynolds-number flows, the viscous effects are confined to a thin layer near the wall boundary and dominated by the viscous terms associated with the strain rate normal to the wall. The terms associated with the strain rates along the body surface are comparatively small. Memory and time constraints make it impractical to demand high grid point densities in both the tangential and streamwise directions to resolve the corresponding derivative components in those viscous terms. The thin-layer Navier–Stokes equations are obtained by eliminating from the full Navier–Stokes equations all viscous terms except those containing derivatives in the direction normal to the body. Thus, from this point of view, the equations selected for this study are the time-dependent compressible thin-layer Navier–Stokes equations. These equations in general body-fitted coordinates (ξ, η, ζ, τ) are[3]

$$\frac{\partial \boldsymbol{Q}}{\partial \tau} + \frac{\partial \boldsymbol{F}_c}{\partial \xi} + \frac{\partial \boldsymbol{G}_c}{\partial \eta} + \frac{\partial \boldsymbol{H}_c}{\partial \zeta} = \frac{\partial \boldsymbol{K}_v}{\partial l} \tag{1}$$

where $\boldsymbol{Q}$ is the conservative variable vector and $\boldsymbol{F}_c$, $\boldsymbol{G}_c$, and $\boldsymbol{H}_c$ are the convective flux vectors in the ξ, η, and ζ directions, respectively. Depending on the block orientation, the viscous flux vector is given by $\boldsymbol{K}_v = \boldsymbol{F}_v, \boldsymbol{G}_v$, or $\boldsymbol{H}_v$ with $l = \xi$, η, or ζ, respectively. In UBIFLOW, the surface normal direction can be either ξ, η, or ζ; thus, the equation shown in Eq. (1) is modified accordingly to yield the thin-layer Navier–Stokes equations for each block.

Numerical Algorithm

UBIFLOW utilizes a finite volume method to ease the imposition of boundary conditions, to inherently uphold the conservative property, and to avoid any grid metric singularity problems. An implicit discretized integral form of Eq. (1) in computational space for a cell (a finite control volume) with center denoted as (i, j, k) is

$$\Delta \boldsymbol{Q}^n + \Delta\tau R^{n+1} = 0 \tag{2}$$

with

$$\Delta \boldsymbol{Q}^n = \boldsymbol{Q}^{n+1} - \boldsymbol{Q}^n$$

$$R^{n+1} = \delta_i(\boldsymbol{F}_c)^{n+1} + \delta_j(\boldsymbol{G}_c)^{n+1} + \delta_k(\boldsymbol{H}_c)^{n+1} - \delta_l(\boldsymbol{K}_v)^{n+1}$$

where $\delta_*( ) = ( )_{*+1/2} - ( )_{*-1/2}$, and the indices i, j, and k are for the ξ, η, and ζ directions, respectively, and n is the temporal index. Again, $\boldsymbol{K}_v = \boldsymbol{F}_v, \boldsymbol{G}_v$, or $\boldsymbol{H}_v$ with $l = i, j$, or k, respectively, depending on the block orientation.

The numerical solution of the nonlinear system of equations given by Eq. (2) is obtained using Newton's method such that

$$[I + \Delta\tau M^{P-1}][\boldsymbol{Q}^P - \boldsymbol{Q}^{P-1}] = -[\boldsymbol{Q}^{P-1} - \boldsymbol{Q}^n + \Delta\tau R^{P-1}] \tag{3}$$

with

$$M^{P-1} = \delta_i\left(\frac{\delta \boldsymbol{F}_c}{\delta \boldsymbol{Q}}\right)^{P-1} \cdot + \delta_j\left(\frac{\delta \boldsymbol{G}_c}{\delta \boldsymbol{Q}}\right)^{P-1} \cdot + \delta_k\left(\frac{\delta \boldsymbol{H}_c}{\delta \boldsymbol{Q}}\right)^{P-1} \cdot - \delta_l\left(\frac{\delta \boldsymbol{K}_v}{\delta \boldsymbol{Q}}\right)^{P-1}$$

The solution of Eq. (3) generates a sequence $\{\boldsymbol{Q}^P\}$ such that as $P \to \infty, \boldsymbol{Q}^P \to \boldsymbol{Q}^{n+1}$.

In UBIFLOW, this formulation is used for both steady-state and unsteady solutions. The Jacobian matrices used in this solution procedure are computed by numerically differentiating the flux vectors. The discretized Jacobians are then used in a Newton-relaxation scheme where a Newton method is the primary iteration, and a relaxation method is the secondary iteration. Formally, Ortega and Rheinboldt[4] refer to this particular solution methodology as a discretized Newton-relaxation method.[5]

Numerical Flux

The flux balance described by the residual term R^{n+1} in Eq. (2) requires that both convective and diffusive fluxes be evaluated at each cell interface. Extrapolations are performed such that a finite difference equivalent of fully upwind or upwind-biased differencing is used for the inviscid (convective) terms, and centered differencing is used for the viscous (diffusive) terms. The inviscid flux is computed using the flux-difference-splitting theory. Summarizing the approach, Roe averaging[6] was used to determine the numerical flux at cell faces, and a variant of the second- or third-order spatial accurate scheme of Osher and Chakravarthy[7] was used. In addition, the van Leer limiter[8] was used for the solutions shown here. For further detailed discussion of the solution algorithms numerical flux function, the reader is referred to Refs. 1 and 9.

The method used to evaluate the viscous flux has been described in detail by Gatlin.[10] The turbulent viscosity μ_t is computed using the algebraic eddy viscosity model due to Baldwin and Lomax.[11] The Baldwin–Lomax turbulence model is applicable for thin viscous layers present in boundary layers of attached flow or a thin shear layer. This turbulence model must be modified for proper use in regions of massive separation, such as those obtained on the leeward side of an elongated body at high angles of attack. The modifications proposed by Degani and Schiff[12] for the calculation of the turbulence model in regions of massive separation was used in this work.

Numerical Simulations

Missile Body at High Incidence Angles

The purpose of this effort was to provide validation and verification of the present thin-layer Navier–Stokes flow solver. The first configuration selected to establish the accuracy of the UBIFLOW solver is that of a missile for which experimental data were available. Flow solutions are presented for a five-caliber tangent ogive missile body referred to as the N3B2 configuration at subsonic high pitch angles. A $145 \times 61 \times 45$ point C-type grid is used to discretize the domain around the body. Minimum cell spacing normal to the surface is about 1×10^{-4} diameters, and a relatively fine grid resolution was maintained within the first diameter in the radial direction. To isolate the effects of the outer boundary, the far-field boundary was placed a distance of 20 diameters from the body. The Mach number was 0.6 for all calculations, and the pitch angle α was varied from 0 to 40 deg. The freestream Reynolds number was 5×10^6 per foot. Local time stepping[1] was used in order to expedite convergence to steady state.

The computed normal-force coefficient C_n for the set of calculations in the range 0 deg $< \alpha <$ 40 deg is compared with the experimental data in Fig. 1 (Ref. 13). For the range 0 deg $< \alpha <$ 30 deg the numerical data are found to be in excellent agreement with experimental data. Beyond 30 deg there is some deviation that is likely caused by the simplicity of the turbulence model and the complexity of the separated flow off of the leeside of the missile. For example, consider the circumferential pressure coefficient C_p distribution at

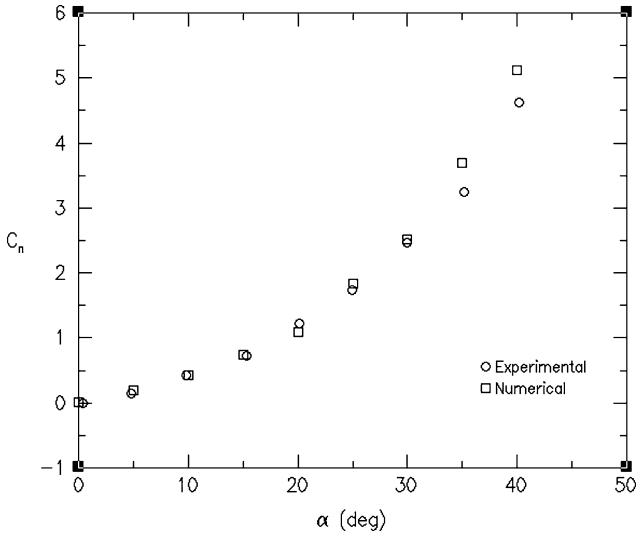

Fig. 1 N3B2 normal-force coefficient.

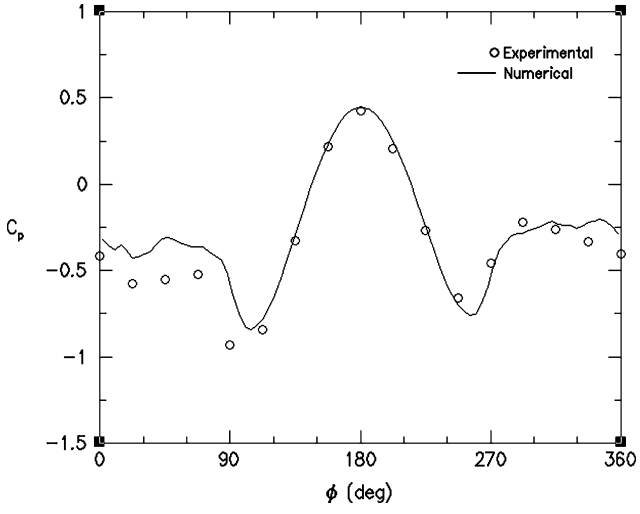

Fig. 2 N3B2 circumferential pressure coefficient distribution for $x/L = 0.82$.

$x/L = 0.82$ shown in Fig. 2 for the N3B2 configuration at an angle of attack of 40 deg. The comparison is quite good on the windward side of the body, yet this far aft the separated flow on the leeward side of the body is not well predicted.

Titan IV Configuration

Performance testing for UBIFLOW toward complex launch vehicle applications was first performed by Whitmire[14] on a buildup of the Titan IV geometry. Whitmire's testing of the Titan IV was for supersonic flow at zero incidence. The geometries studied were made more complex by sequentially adding components of the Titan IV vehicle, running a simulation, and comparing local C_p data to experiment. The results of those tests gave a good indication of the significance each appendage has in accurately predicting the pressure distribution over the overall complex geometry. UBIFLOW was further tested by solving for the flow over the complete Titan IV A-model geometry at pitch and yaw angles. The results of those tests are presented here.

The configuration simulated for this effort consisted of a payload fairing (PLF), the core vehicle, two solid rocket motors (SRM), two staging motor fairings (SMF), and two thrust-vector-control (TVC) tanks. To obtain accurate viscous solutions, a smooth relatively orthogonal grid had to be generated. This was a difficult task, considering the complexity of the multibody configuration and the close proximity of interacting components. The grid generation for the Titan IV configuration was done with the GUM-B (general unstructured multiblock) grid-generation tool.[15] This software tool is a general three-dimensional algebraic/elliptic grid-generation system that generates both the boundary surfaces and the interior grid. The grid generator uses a multiblock scheme to handle the geometric complexities.

The grid was comprised of 52 blocks containing approximately 2.5 million grid points. The block system for this configuration consists of a C-O grid enclosing the PLF, TVC, and SRM, with an H-O grid surrounding the SMF and the embedded C-O structure. Away from the body, a C-O type system extends from the nose of the C-O type system surrounding the body out to the upstream external boundary. The far-field boundaries were placed 15 PLF body lengths upstream of the nose of the PLF and outboard of the PLF. Similar to the wind-tunnel model, the geometry was simulated with a sting attached to the core vehicle. The Mach number was 0.6 for all calculations shown here. At the incidence angles tested, this is above the critical Mach number for this vehicle. Independently, the pitch angle α and the yaw angle β were varied from 0 to 10 deg. Also, the freestream Reynolds number was 3×10^6 per foot. Again, local time stepping was used in order to expedite convergence to steady state.

The computed normal-force coefficient C_n for the set of calculations in the range 0 deg $< \alpha <$ 10 deg is compared with available experimental data in Fig. 3 (Ref. 13). For the normal-force coefficient, the comparison with experimental data appears to be quite good. The source of the slight disagreement in the normal force is thought to be a combination of the absence of the electric cable fairing from the simulation, and that the numerical-force coefficient in the figure was generated by integrating pressure only. In subsequent work, it was found that the viscous contribution added about 2–3% to the total normal force. A detailed review of flowfield visualization reveals that the interaction of the various components is only slightly related to wake impingement as a result of the side-by-side arrangement of the largest components of the configuration. The pitch simulations do generate slight forces in the yaw (sideslip) direction (on the order of a few percent of the normal force), which is thought to be caused by the asymmetries of the launch vehicle.

In Fig. 4, the computed side-force coefficient C_y for the set of calculations in the range 0 deg $< \beta <$ 10 deg is compared with available experimental data.[13] Unlike the normal-force comparison, the side-force comparison does not indicate as good agreement with the experiment. This is likely because of the separated flow of the upstream components impinging on downstream components. For example, in sideslip, the flow separating off the SRM impinges on the core vehicle, and then impinges on the other SRM farther aft. The complexity of this interaction increases as the angle of incidence increases, and thus the applicability of the simple algebraic turbulence model used here can come into question. Grid resolution

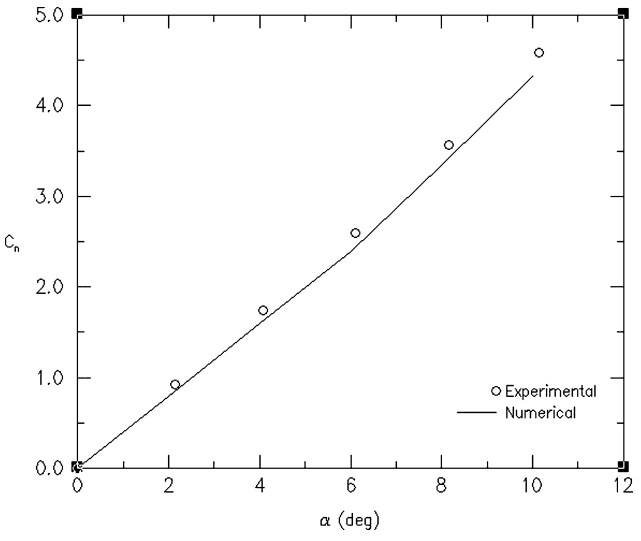

Fig. 3 Titan IV normal-force coefficient.

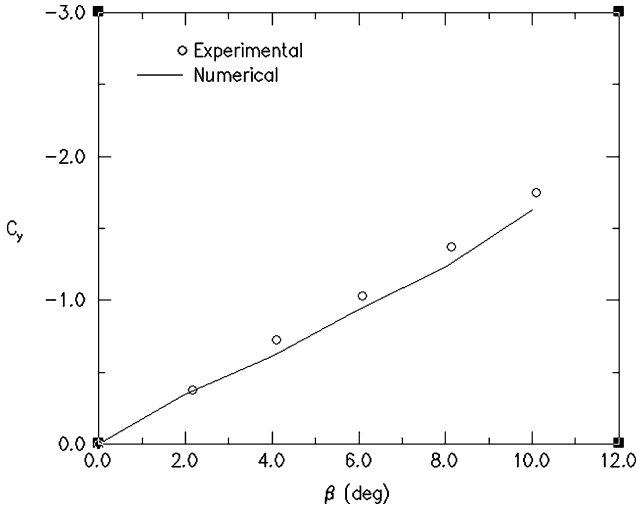

Fig. 4 Titan IV side-force coefficient.

might be an issue in the regions of flow separation as it is impossible to know a priori the origins and trajectories of the multiple vortices trailing off the many components of the vehicle. Similar to the pitch simulations, the yaw simulations generated slight forces in the pitch direction as a result of the asymmetries of the vehicle.

Conclusions

The flow solver, UBIFLOW, was developed with the goal of producing efficient, accurate flow solution software capable of handling complex configurations. In the work presented here, UBIFLOW's ability to simulate the flowfield of complex configurations was tested on a couple of launch vehicles. The predictive capability of UBIFLOW was demonstrated through the use of sample launch configurations for which experimental data were available. Computational results were presented for these high-incidence-angle configurations in the transonic speed regime to evaluate the accuracy and reliability of the UBIFLOW code. Considering the assumptions in the viscous model used in this study, that is, the thin-layer assumption and the simple algebraic turbulence model, the agreement with experimental data is thought to be excellent for the pitch simulations and good for yaw simulations.

Acknowledgments

The authors thank Lockheed Martin Corp. and Victor Whitehead for supporting this effort. In addition, Peter Huseman, our Technical Monitor, is to be credited with steering us in the direction of high incidence angle maneuvers. The authors also thank Joe Bomba of Lockheed Martin for his assistance in acquiring geometry and experimental data and in reducing the raw numerical data for comparison.

References

[1]Arabshahi, A., "A Dynamic Multiblock Approach to Solving the Unsteady Euler Equations About Complex Configurations," Ph.D. Dissertation, Dept. of Aerospace Engineering, Mississippi State Univ., Mississippi State, MS, May 1989.

[2]Thomas, P. D., and Lombard, C. K., "Geometric Conservation Law and Its Application to Flow Computations on Moving Grids," *AIAA Journal*, Vol. 17, No. 10, 1979, pp. 1030–1037.

[3]Tannehill, J. C., Anderson, D. A., and Pletcher, R. H., *Computational Fluid Mechanics and Heat Transfer*, 2nd ed., Taylor and Francis, Washington, DC, 1997.

[4]Ortega, J. M., and Rheinboldt, W. C., *Iterative Solution of Nonlinear Equations in Several Variables*, Academic Press, New York, 1970.

[5]Vanden, K. J., "Direct and Iterative Algorithms for Three-Dimensional Euler Equations," Ph.D. Dissertation, Dept. of Aerospace Engineering, Mississippi State Univ., Mississippi State, MS, Dec. 1992.

[6]Roe, P. L., "Approximate Riemann Solvers, Parameter Vectors, and Difference Schemes," *Journal of Computational Physics*, Vol. 43, No. 2, 1981, pp. 357–372.

[7]Osher, S., and Chakravarthy, S., "Very High Order Accurate TVD Schemes," ICASE Rept. 84-44, Sept. 1984.

[8]van Leer, B., "Toward the Ultimate Conservative Difference Scheme. V. A Second Order Sequel to Godunov's Method," *Journal of Computational Physics*, Vol. 32, No. 1, 1979, pp. 101–136.

[9]Whitfield, D. L., Janus, J. M., and Simpson, L. B., "Implicit Finite Volume High Resolution Wave-Split Scheme for Solving the Unsteady Three-Dimensional Euler and Navier–Stokes Equations on Stationary or Dynamic Grids," Engineering and Industrial Research Station, Mississippi State Univ., Rept. MSSU-EIRS-ASE-88-2, Mississippi State, MS, Feb. 1988.

[10]Gatlin, B., "An Implicit, Upwind Method for Obtaining Symbiotic Solutions to the Thin-Layer Navier–Stokes Equations," Ph.D. Dissertation, Dept. of Mechanical and Nuclear Engineering, Mississippi State Univ., Mississippi State, MS, Aug. 1987.

[11]Baldwin, B. S., and Lomax, H., "Thin-Layer Approximation and Algebraic Model for Separated Turbulent Flows," AIAA Paper 78-257, Jan. 1978.

[12]Degani, D., and Schiff, L. B., "Computation of Turbulent Supersonic Flow Around Pointed Bodies Having Crossflow Separation," *Journal of Computational Physics*, Vol. 66, No. 1, 1986, pp. 173–196.

[13]Arabshahi, A., and Janus, J. M., "A Multiblock Compressible Navier–Stokes Solver Applied to Complex Launch Vehicles," AIAA Paper 99-3378, June–July 1999.

[14]Whitmire, J. B., "A Numerical Simulation of the Lockheed-Martin Titan IV Booster," M.S. Thesis, Dept. of Aerospace Engineering, Mississippi State Univ., Mississippi State, MS, May 1995.

[15]Remotigue, M., and Jiang, M. Y., "GUM-B Grid Generation Code and Applications," *Proceedings of the 6th International Conference*, edited by M. Cross, B. K. Soni, J. F. Thompson, J. Hauser, and P. R. Eiseman, International Society of Grid Generation, NSF Engineering Center for Computational Field Simulation, College of Engineering, Mississippi State Univ., Mississippi State, MS, 1998, pp. 823–832.

R. Cummings
Associate Editor

Parametric Scaling Model for Nongeosynchronous Communications Satellites

Philip N. Springmann* and Olivier L. de Weck†
Massachusetts Institute of Technology, Cambridge, Massachusetts 02139

Nomenclature

g	=	acceleration caused by gravity, m/s^2
I_{sp}	=	specific impulse, s
M_{dry}	=	spacecraft dry mass, kg
M_{PL}	=	payload mass, kg
M_{pp}	=	primary power mass, kg
M_{prop}	=	propellant mass, kg
M_{wet}	=	spacecraft wet mass, kg
M_0	=	premaneuver spacecraft mass, kg
N	=	number of data points
P_{bol}	=	total power at beginning of life, W
P_{eol}	=	total power at end of life, W
P_{PL}	=	payload power, W

Presented as Paper 2003-2310 at the 21st International Communications Satellite Systems Conference, Yokohama, Japan, 15–19 April 2003; received 3 November 2003; revision received 19 February 2004; accepted for publication 25 February 2004. Copyright © 2004 by Philip N. Springmann and Olivier L. de Weck. Published by the American Institute of Aeronautics and Astronautics, Inc., with permission. Copies of this paper may be made for personal or internal use, on condition that the copier pay the $10.00 per-copy fee to the Copyright Clearance Center, Inc., 222 Rosewood Drive, Danvers, MA 01923; include the code 0022-4650/04 $10.00 in correspondence with the CCC.

*Undergraduate Research Assistant, Department of Aeronautics and Astronautics. Student Member AIAA.

†Assistant Professor, Department of Aeronautics and Astronautics, Engineering Systems Division. Member AIAA.